Isolation and Structure Elucidation of the Major Degradation Products of Cefaclor Formed under Aqueous Acidic Conditions

STEVEN W. BAERTSCHI,[X] DOUGLAS E. DORMAN, JOHN L. OCCOLOWITZ, MONTE W. COLLINS, LARRY A. SPANGLE, GREGORY A. STEPHENSON, AND LESLIE J. LORENZ

Received October 15, 1996, from the *Lilly Research Laboratories, Eli Lilly and Company, Lilly Corporate Center, Indianapolis, IN 46285.* Final revised manuscript received January 27, 1997. Accepted for publication February 7, 1997[⊗].

Abstract □ The aqueous acidic degradation of the oral cephalosporin cefaclor was investigated. A number of degradation products were isolated and characterized. The degradation products can be loosely classified into three categories: thiazole derivatives, pyrazine derivatives, and simple hydrolysis or rearrangement products. Degradation pathways are proposed that involve (1) hydrolysis of the β-lactam carbonyl with subsequent rearrangement, (2) ring contraction of the six-membered cephem nucleus to five-membered thiazole derivatives through an episulfonium ion intermediate, and (3) attack of the primary amine of the phenylglycyl side chain on the "masked aldehyde" at carbon-6 to form fluorescent substituted pyrazines.

Introduction

Knowledge of the structures of degradation products and the degradation pathways by which they arise are an important part in the understanding of the chemistry, stability, and activity of drug products. For this reason, we investigated the degradation pathways of the oral cephalosporin cefaclor (**1**) and recently characterized a novel aqueous degradation product (**2**).[1] The structure of **2** revealed a prominent acidic degradation pathway involving a ring-contraction from a six-membered cephem ring to a five-membered thiazole ring. This new pathway of cefaclor degradation is distinct from the previously established degradation pathway leading to 2-hydroxy-3-phenyl pyrazine (**3**).[2]

Examination of acidic aqueous degradations (degradations in 0.1 N HCl and in unbuffered water) of cefaclor by high-performance liquid chromatography (HPLC) reveals numerous degradation products (see Figures 1−3). This report details the isolation and characterization of the major degradation products of cefaclor arising under acidic aqueous conditions, along with proposals for pathways by which they form. Evidence is presented for a generalized pathway to fluorescent degradation products.

Experimental Section

The solutions of cefaclor described were periodically monitored by HPLC for degradation. The degradation profile was examined to ensure that the major degradation product levels were increasing so that isolation by preparative HPLC would be facilitated.

Degradation of Cefaclor—*0.1 N HCl Degradation*—Cefaclor (95 g) was dissolved in 19 L of 0.1 N HCl and stored in a glass container with a loose aluminum foil cover at room temperature. The solution was allowed to degrade for 2 months prior to isolation of the degradation products by preparative reversed-phase (rp)-HPLC. At this point, ~85% of the cefaclor had degraded as determined by analytical rp-HPLC (Figure 1). The compounds formed under these conditions were isolated and purified by the preparative HPLC procedures described in the next section. The degraded solution also contained a precipitate that was isolated by filtration and subsequently identified as elemental sulfur.[1]

Unbuffered Water Degradation—Cefaclor (95 g) was dissolved in 19 L of deionized water, stored in a glass container with a loose aluminum foil cover, and allowed to degrade at room temperature for 9 months prior to isolation of the degradation products. At this point, >90% of the cefaclor had degraded as determined by analytical rp-HPLC (Figure 2). During this degradation, the acidity of the solution changed from pH ~6 to pH 2.75. Two compounds formed under these conditions were isolated and purified by the preparative HPLC procedures described (**11** and **13**). The degraded solution also contained a precipitate that was identified as elemental sulfur.

Degradation at pH 5.5—Cefaclor (200 g) was dissolved in 20 L of water, the solution was stored in a glass container with a loose aluminum foil cover, and the pH of the solution was adjusted to 5.5 with 5 N NaOH (the pH 5.5 degraded solution). The pH was adjusted daily to ~5.5 with 5 N NaOH to counteract the tendency of the solution to become more acidic. The pH was maintained between 4.8 and 6.0 during the course of the degradation. After 3 months at room temperature, cefaclor was shown by HPLC analysis to be ~87% degraded (Figure 3). The solution was fractionated by the preparative HPLC procedures described in the next section. Two fractions, those containing **8** and **14**, were further purified and characterized. In addition to these compounds, elemental sulfur was present as a precipitate in the solution. The relative amount of elemental sulfur was higher in the pH 5.5 solution than in the acidic solutions in which cefaclor was degraded.

HPLC—*Analytical*—The analytical scale rp-HPLC system utilized a photodiode array detector to detect eluting peaks (deuterium lamp; wavelength accuracy, ±1.0 nm adjusted to the line spectrum of the deuterium lamp at 656.1 nm; UV detection from 200 to 400 nm at 4-nm resolution; 1-s interval between acquisition of successive spectra; Waters 990, Milford, MA). The HPLC was run in a gradient mode from 0 to 100% solvent B in 30 min and held at 100% solvent B for 10 min. Solvent A was an aqueous solution containing 2.4 g/L NaH_2PO_4 and 1 mL of H_3PO_4 per liter. Solvent B was a mixture of 60% acetonitrile and 40% solvent A (v/v). The flow rate was 1.0 mL/min. An octyldecyl silane (ODS) rp-HPLC column was used (4.6 × 250 mm, 5 μM, YMC, Wilmington, NC).

Preparative—The degraded solutions of cefaclor just described were separated into 20 fractions by an automated HPLC and fraction collection system. The sample solutions were placed in a pressurized container, and aliquots of the sample were automatically injected onto the column through a 10-mL sample loop. The system used a C-18 semipreparative rp-HPLC column (20 × 250 mm, 5 μM, YMC, Wilmington, NC). The HPLC was run in a gradient mode from 0 to 100% solvent B in 35 min and held at 100% solvent B for 7 min. Solvent A was an aqueous solution of 0.1% acetic acid, and solvent B

[⊗] Abstract published in *Advance ACS Abstracts,* April 1, 1997.

S0022-3549(96)00427-3 CCC: $14.00

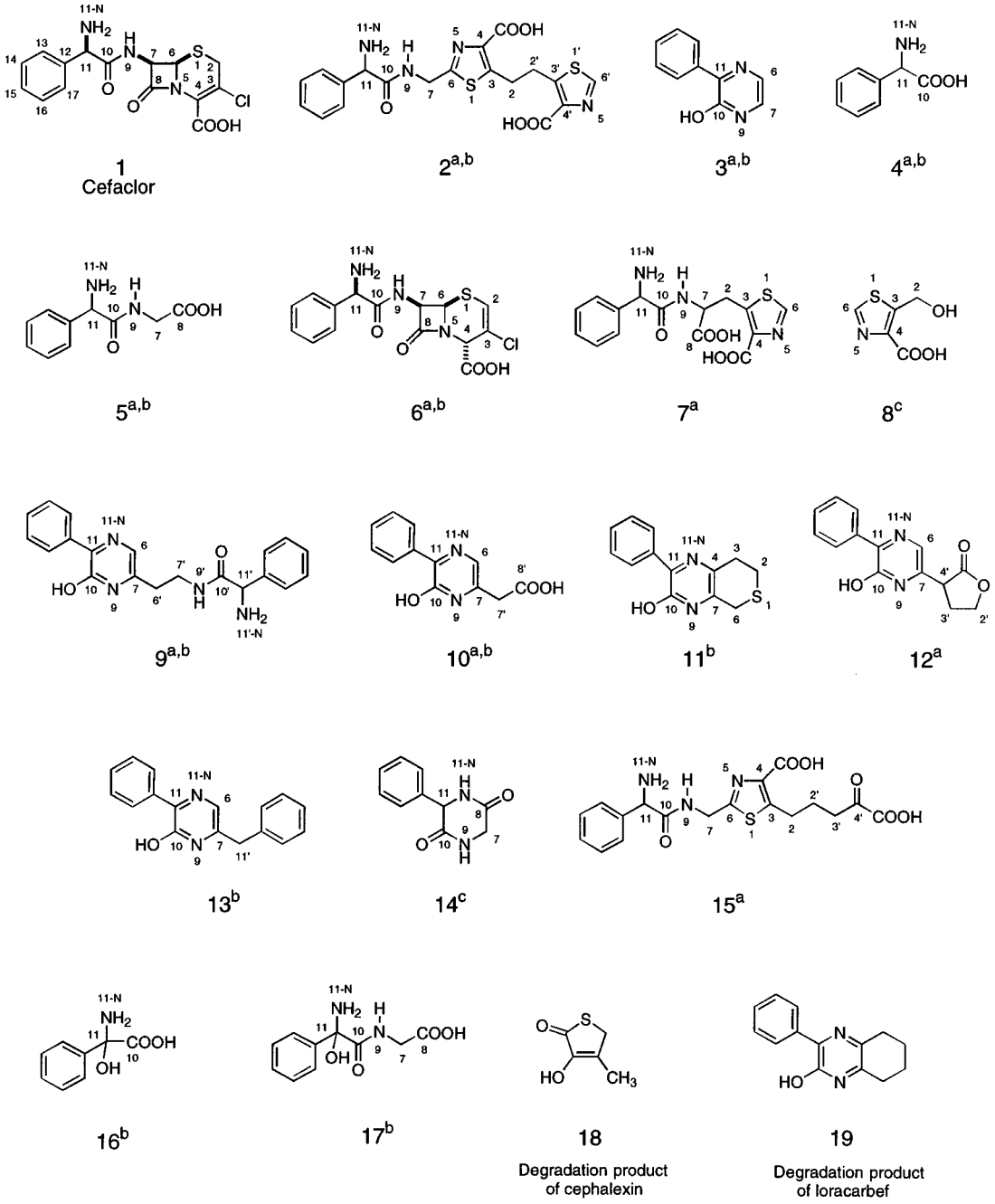

Chart 1—[a]0.1 N HCl degradation product. [b]Deionized water degradation product. [c]pH 5.5 degradation product.

consisted of a mixture of 60% acetonitrile and 40% solvent A (v/v). The flow rate was 10 mL/min. Fraction collector advance times were determined manually. A total of 78, 117, and 45 preparative injections were made for fractionation of the 0.1 N HCl, the unbuffered, and the pH 5.5 degraded solutions, respectively. In each case, the solvent was removed by lyophilization.

Selected fractions were further purified by rp-HPLC prior to spectroscopic analysis. These fractions were re-dissolved in a solution of 0.1% acetic acid and acetonitrile and purified by rp-HPLC (20 × 250 mm column as already described) using appropriate isocratic solvent systems ranging between 5 and 80% solvent B. In this second purification step, fractions of interest were collected manually. This collection was guided by observation of the UV response at 220 nm. The collected fractions were immediately cooled to 0 °C by placing them on ice. The solvent was removed by lyophilization. The purities of these fractions were assessed by analytical rp-HPLC already described.

Sources of Known Compounds—Chemical shifts of carbons and protons of the known compounds described next are tabulated in Table 1. All data in this table were measured in the dimethyl sulfoxide/trifluoroacetic acid (DMSO/TFA) solvent system described later.

*2-Hydroxy-3-phenylpyrazine (**3**)*—Compound **3** was obtained from synthesis as described previously.[1]

D-Phenylglycine (***4***)—Compound **4** was obtained from the Aldrich Chemical Company, Milwaukee, WI.

D-Phenylglycyl-glycine (***5***)—*t*-Butyloxycarbonyl-D-phenylglycine (1 mmol) and 1-hydroxybenzotriazole (1 mmol) were dissolved in 50 mL of dichloromethane at room temperature. One equivalent of dicyclohexylcarbodiimide (206 mg) was added, and the solution was stirred for 2 h. A white precipitate was formed and removed by filtration. *t*-Butylglycinate (1 mmol) was then added and the solution was allowed to stir overnight at room temperature. The solution was then successively washed with 0.1 N HCl, $NaHCO_3$ (0.02 g/mL), 1 N NaOH, and 0.1 N HCl. The organic phase was separated and then evaporated under reduced pressure. The reaction product was dissolved in a solution of TFA (5 mL) and triethylsilane (1 mL). After 1 h, the TFA/triethylsilane was removed under reduced pressure at room temperature. Addition of ~50 mL of diethyl ether yielded a white solid,

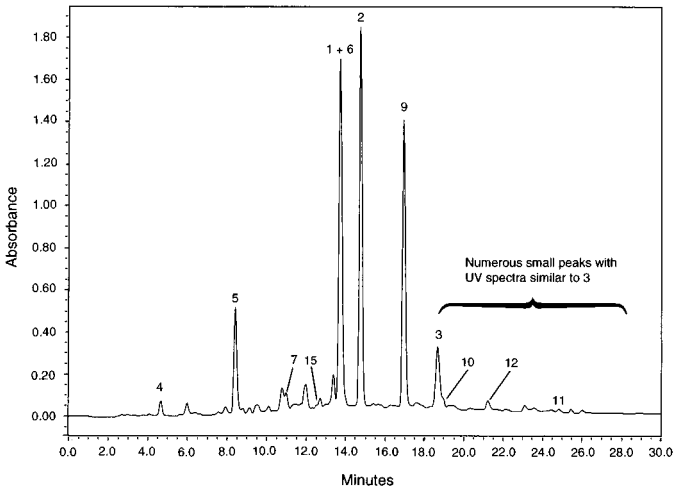

Figure 1—rp-HPLC chromatogram (UV, 220 nm) of a solution of cefaclor stored for 2 months at room temperature in 0.1 N HCl. See *Experimental Section* for chromatographic details.

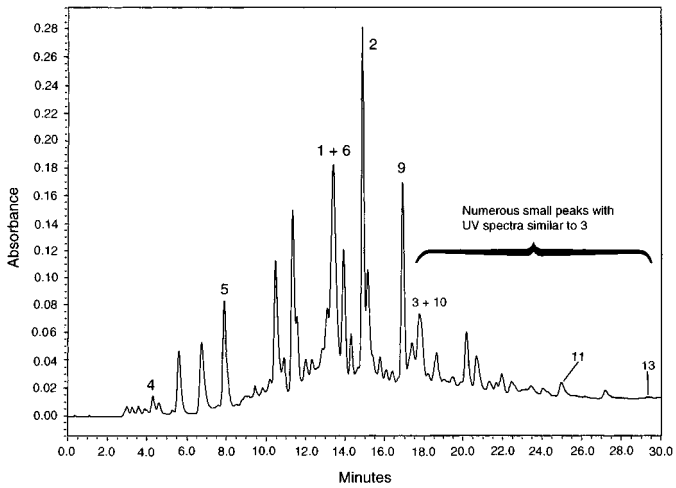

Figure 2—rp-HPLC chromatogram (UV, 220 nm) of a solution of cefaclor stored in deionized water for nine months at room temperature. See *Experimental Section* for chromatographic details.

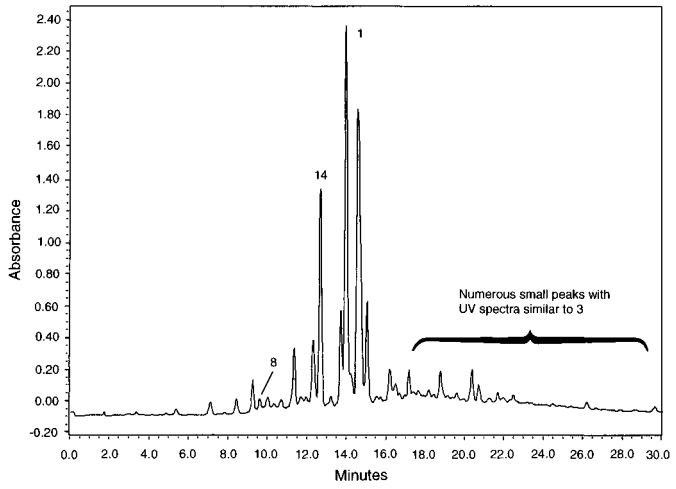

Figure 3—rp-HPLC chromatogram (UV, 220 nm) of a solution of cefaclor stored at room temperature for 2 months at a pH maintained between 4.8 and 6.0. See *Experimental Section* for chromatographic details.

which was collected by filtration and washed with diethyl ether. The total weight of recovered product was 120 mg (0.37 mmol) for a 37% overall yield. The product was purified by rp-HPLC (as already described) and analyzed by probe electron-impact mass spectroscopy (EI-MS), fast atom bombardment MS (FAB-MS), and proton nuclear magnetic resonance spectroscopy (^{1}H NMR). FAB-MS showed an MH^+ of m/z 209; the highest mass ion observed by EI-MS was m/z 190 (208−18, ring-closure and dehydration on the heated probe). The sample showed major fragments at m/z 147, 132, 118, 106, 104, 91, 79, and 77. For NMR assignments see Table 1.

*2-Hydroxy-3-phenyl-5-benzylpyrazine (**13**)*—The preparation of **13** was performed according to the procedure of Barbhaiya.[3] Cephalexin (100 mg, Eli Lilly and Company) in distilled water (100 mL) was treated (10 min, room temperature) with NaOH solution (50 mL, 1 N). Then HCl (50 mL, 1 N) was added, followed by Sorensen's citrate buffer (300 mL) containing benzaldehyde (1.0% v/v). The pH of the buffer was adjusted to 5.0 and then the buffer was heated at 100 °C for 30 min, cooled, and extracted repeatedly with ethyl acetate. The combined organic layers were evaporated, and the product was purified by crystallization from ethyl acetate. For NMR assignments see Table 1.

*Δ^2-Cefaclor (**6**)*—Cefaclor·*N,N*-dimethylformamide disolvate (250 g, obtained from Eli Lilly and Company) was added to a 5-L 3-necked round-bottomed flask containing 2500 mL of dimethylformamide and fitted with a mechanical paddle stirrer. After stirring for 15 min, 2.5 eq (298 mL) of bis(trimethylsilyl)acetamide (BSA) was added, followed by addition of 2.5 eq of triethylamine (TEA, 170 mL) and stirring for 10 min. At this point, the solution was a ~50:50 mixture of tetramethylsilane (TMS)-protected cefaclor and Δ^2-cefaclor. Hydrolysis of the TMS-protecting groups and precipitation of cefaclor was accomplished by rapid addition of 250 mL of 6 N HCl, which lowers the pH to ~5.2. After 30 min, the pH dropped to ~4.1, and was adjusted to ~5.7 via dropwise addition of TEA. The temperature was reduced to 10 °C by submerging the flask in an ice bath, and the cefaclor precipitate was removed by filtration. Δ^2-Cefaclor was crystallized from the solution by adding two volumes of acetone. The crystalline precipitate was recovered by filtration and washed with acetone, cold water, and acetone. Solvent removal was accomplished by placing the product under reduced pressure at room temperature for ~72 h. Overall yield was: 19% (47.5 g). HPLC analysis of the final product revealed <1% contamination by the parent cefaclor. FAB-MS indicated the protonated molecular ion to be m/z 368. FAB-MS/MS measurements of m/z 368 revealed a fragmentation pattern similar to that of cefaclor. The UV spectrum of Δ^2-cefaclor has a characteristic "double-humped" appearance (λ_{max}values at ~240 and 260 nm, Figure 4). The fully assigned ^{1}H and ^{13}C NMR spectra (see Table 1) were consistent with the proposed structure. In the ^{1}H NMR spectrum, the resonances of the protons at sites 6, 7, and 9 had the characteristic three-spin pattern of β-lactams, and H-2 and H-4 were coupled by 1.5 Hz, as is typical of Δ^2-cephalosporins.[4]

Δ^2-Cefaclor dihydrate was crystallized by evaporation from an acetonitrile/water mixture in the monoclinic space group *C*2 (No. 5) with unit cell parameters and calculated volume of $a = 26.939$ (5), $b = 7.551$ (1), $c = 9.704$ (2), $\beta = 109.23$ (2)°, and $V = 1863.9$. The calculated density is 1.44 g·cm^{-3} for $Z = 4$ and a formula weight of 403.84 The data were collected on a Enraf-Nonius CAD4 diffractometer using CuK_α radiation and a graphite monochromator. A total of 2099 reflections were collected, of which 2053 were unique. The structure was solved by direct methods using the SIR92[5] program. The remaining atoms were located in succeeding difference Fourier syntheses. SHELX-93 was used for structure refinement.[6] The highest peak in the final difference Fourier map was 0.71 $e{\cdot}A^{-3}$. Anisotropic temperature factors were assigned to all nonhydrogen atoms, but the hydrogens were kept isotropic. Full-matrix least-squares refinement of all nonhydrogen coordinates and thermal parameters gave final factors $R = 5.2\%$ and $Rw = 14.3\%$. Complete tables of the fractional coordinates, bond angles, and bond lengths are provided in the supplement.

Measurement of Spectra—*UV Spectra*—UV spectra were acquired by the HPLC photodiode array-UV system (already described) as the peaks eluted off the analytical column.

IR Spectra—FT-IR spectra of the samples were obtained with a SpectraTech IR PlanII FT-IR microscope in conjunction with a Nicolet model 60 SXB FT-IR spectrometer. Typically, several particles of the sample totaling <50 μg were placed on a 13-mm diameter potassium bromide disk. The particles were then flattened with a microspatula to provide a sample of suitable thickness.

Mass Spectra—FAB-MS and FAB-MS/MS data were obtained with a VG ZAB-3 (B_1EB_2) triple-sector mass spectrometer or a VG ZAB-

Table 1—^{13}C and ^{1}H NMR Chemical Shifts for Isolated Degradation Products[a]

site:	4	8[b]	3	14	5	10[c]	11	12	13[d]	9[e,f]	7[e]	6	2[g]
2		n.o.					25.50				n.o.	118.23	28.15[k]
		5.11					2.96				3.71,3.56	6.75	3.48
3		n.o.					25.50				n.o.	113.83	147.12[j]
							2.96				2.96	2.96	2.96
4		n.o.					n.o.				n.o.	54.02	142.72[h]
							2.96				2.96	4.87	4.87
4-COOH		n.o.									n.o.	167.28	163.22[j]
6		n.o.	126.80			122.20	31.04		122.60	122.75	n.o.	52.64	164.24
		8.85	7.40			7.26	3.68		7.43	7.18	8.57	5.18	5.18
7			123.09	44.24	41.06	137.73	n.o.	n.o.	140.43	139.07	n.o.	59.94	40.65
			7.47	3.94,3.74	3.82	3.82	3.82	7.74	7.74	7.74	4.57	5.62	4.54
8				165.85[h]	170.56			n.o.			n.o.	163.37	
9	10.77			8.13	8.85						n.o.	9.64	n.o.
10	174.24		155.28	166.89[h]	167.79	155.57	154.12	n.o.	155.85	155.85	n.o.	168.09	167.86
11	61.23		151.57	58.60	55.47	147.82	129.00	n.o.	148.30	148.13	n.o.	55.50	55.73
	5.16		5.16	4.87	5.05	5.05	5.05	5.05	5.05	5.05	~4.9	5.06	5.01
11-NH	8.40			8.61	9.5						n.o.	8.84	n.o.
12	136.11		136.06	138.86	134.1	136.28	135.87	n.o.	136.08	136.17[h]	n.o.	133.53	133.62
13,17	126.74		128.24	126.85	128.12	127.82	127.82	n.o.	128.16	127.73[i]	n.o.	127.94	128.17
	7.38		8.31	7.36	7.54	8.21	8.25	8.22	8.30	8.29	7.4–7.25	7.54	7.54
14,16	128.68		127.76	128.58	128.82	128.03	128.31	n.o.	127.82	128.18[i]	n.o.	128.88	129.45
	7.38		7.44	7.36	7.42	7.34	7.43	7.43	7.43	7.38	7.4–7.25	7.44	7.44
15	128.29		129.36	127.90	129.24	129.00	129.20	n.o.	129.13	128.96[j]	n.o.	129.44	128.92
	7.38		7.44	7.36	7.45	7.34	7.43	7.43	7.40	7.29	7.4–7.25	7.44	7.44

[a] Each cell of the table contains the carbon (top line) and proton (bottom line) chemical shift(s); unless otherwise noted, all spectra were measured in DMSO-d_6/TFA; compounds are numbered to reflect their most probable mechanistic origin fom cefaclor, which is numbered as shown in **1**; n.o., not observed. [b] Measured in perdeuteromethanol. [c] 7′: 15.84/2.14; 8′: n.o. [d] CH_2: 35.60/3.88; *ipso*:137.36/-; *ortho*:128.84/7.38; *meta*:128.63/7.35; *para*: 126.84/7.26. [e] Measured in DMSO-d_6. [f] 6′: 29.72/2.64; 7′: 37.26/3.43; 9′: n.o.; 10′: 170.92; 11′: 57.58/4.56; 11′-NH_3: n.o.; 12′: 138.81[h]; 13′,17′: 127.06[i]/7.4; 14′,16′: 128.01[i]/7.4; 15′: 127.66[i]/7.4. [g] 2′: 141.60/-[h]; 3′: 146.69/- [j]; 4′: 28.58/3.48[k]; 4′-COOH: 163.01[i]/-; 6′: 151.22/8.91. [h–k] Assignments within a single column may be interchanged.

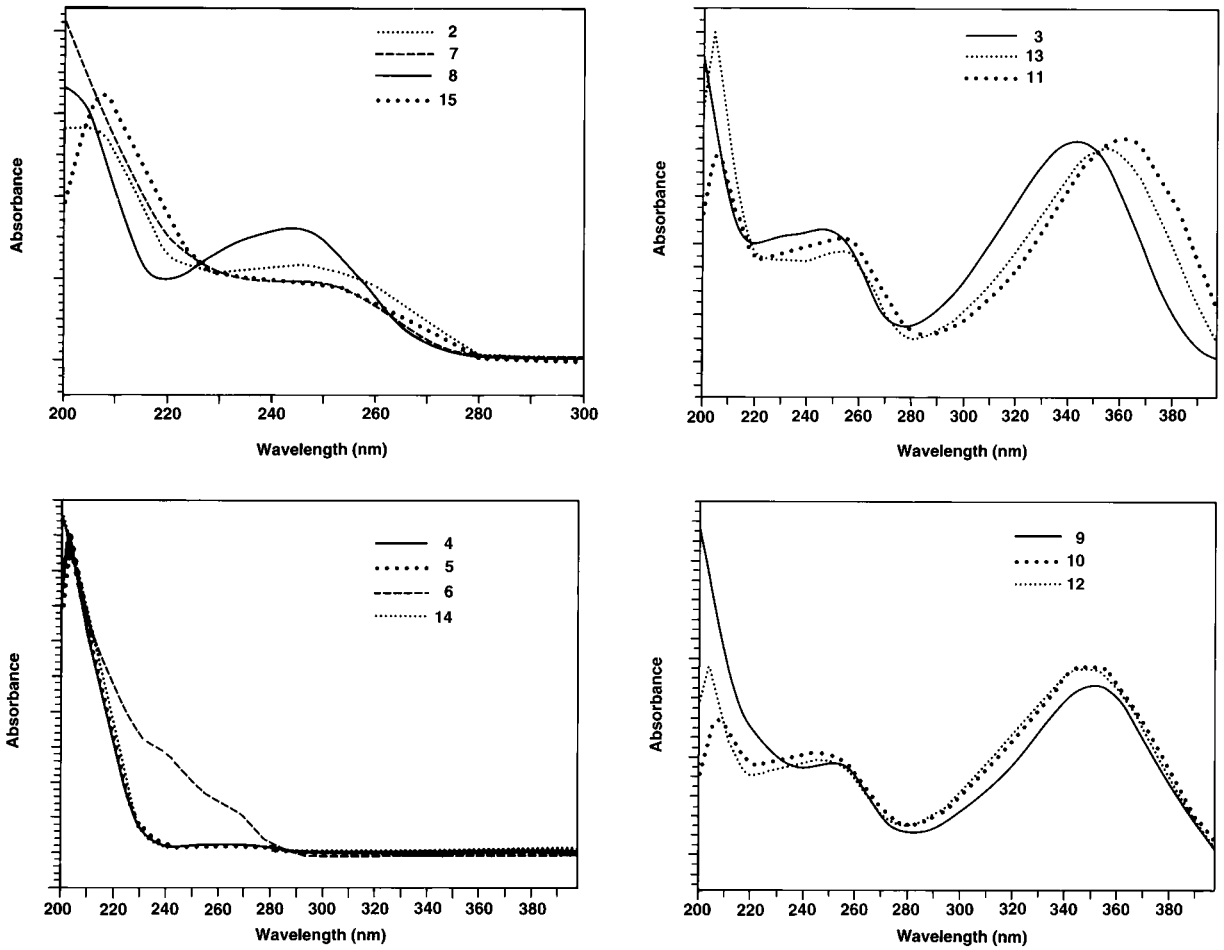

Figure 4—UV spectra of cefaclor degradation products obtained on the photodiode array-UV detector as the compounds eluted from the column.

2SE (BE) two-sector mass spectrometer. Samples were dissolved in "Magic Bullet" (a 5:1 solution of dithiothreitol:dithioerythritol in methanol) and bombarded with 8 KeV xenon atoms in the ZAB-3 or Cs ions, with a net energy of 12 KeV, in the ZAB-2SE. For MS/MS experiments with the ZAB-3, the precursor ions were selected with B_1 and collisionally activated (50% attenuation using He collision gas)

in the second field-free region. The products were separated by a constant B_2/E linked-scan. For MS/MS experiments using the ZAB-2SE, the ions leaving the ion source were collisionally activated with helium in the first field-free region and the products were separated with a constant B/E linked-scan.

NMR Spectra—^{1}H and ^{13}C NMR spectra were recorded on Bruker AC-250 or AMX-500 spectrometers. Spectra were recorded in DMSO-d_6 and referenced to internal TMS on the bases of the chemical shifts of residual solvent peaks. In some cases the peaks of the initial spectrum recorded were broad, and in these cases the addition of a trace of TFA sharpened the spectra significantly, presumably due to the conversion of a mixture of protonation states to the TFA salt. The use of this solvent system also permitted the observation of the protons at exchangeable sites, such as ammonium ions. The multiplicities of the carbon resonances were determined by the DEPT method.[7] Carbon–proton correlations were detected by two-dimensional heteronuclear experiments designed to detect correlations due to coupling through one[8] or more than one[9] chemical bond. Chemical shift data for all compounds for which NMR spectra were measured appear in Table 1. ^{1}H NMR spectra were modeled using the Bruker program PANIC.

Derivatizations—Derivatizations with diazomethane were accomplished as previously described.[1]

Results

Elucidation of Structures—Because all the compounds isolated from these degradations are related structurally, some generalities can be stated about their properties and spectra. For example, many of the compounds isolated in this research include the phenylglycyl substructure. This substructure was found to be associated with two fragments in the FAB-MS/MS spectrum:

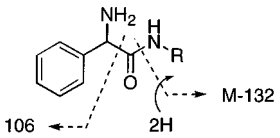

The first fragment results from benzylic cleavage to give a fragment at m/z 106. The second fragment results from cleavage of the amide bond with loss of the phenylglycyl group from the protonated molecular ion to yield a fragment m/z M − 132. In the UV spectrum, the phenylglycyl group contributes primarily to end absorbance, but also includes a weak phenyl chromophore at ~260 nm (see UV spectra of **4**, **5**, and **14**, Figure 4). In the NMR spectra, the phenylglycyl group contributes peaks due to the phenyl ring and to a methine with carbon and proton shifts at approximately δ 55.5 and 5.05, respectively (see Table 1). The last resonance is typically coupled to the three-proton resonance of the NH_3^+ group near δ 8.7 when the ^{1}H NMR spectrum is measured in DMSO with added TFA (see *Experimental Section*). Correlation of the carbon and proton resonances through their two- and three-bond couplings[9,10] can be used to extend this substructure further. For example, the amide carbonyl resonance, which can be identified by its correlations to H-11 and the protons of the NH_3^+ group, is also generally correlated to the amide NH and the proton(s) on carbon 7. This permits the definition of connectivity between the phenylglycine moiety and the remainder of the molecule.

Another common type of degradation product encountered in this research contained the 2-hydroxy-3-phenylpyrazine substructure.[2] The UV spectra of these compounds are quite distinctive, showing significant absorbances in the regions 240–260 and 330–370 nm (see UV spectra of **3**, **11**, and **13**, Figure 4). These compounds are also characterized by ^{1}H NMR spectra including a two-proton multiplet near δ 8.3, assigned to the *ortho* protons of the phenyl ring. The other aromatic protons, including any on the pyrazine ring, all

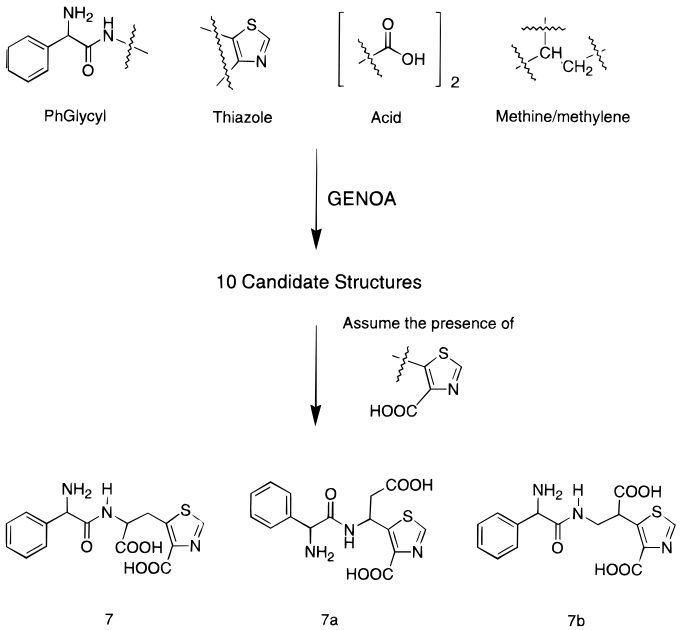

Figure 5—Illustration of the structural possibilities as determined with the indicated substructural units and the computer program GENOA. From the indicated substructures, GENOA constructed 10 possible structures. The assumption that the molecule retains the 4-carboxylthiazol-5-yl substructure reduced this list to three candidates.

generally group together at about δ 7.45. In the mass spectra, this substructure is often found to lose a benzonitrile fragment.[11]

Several of the degradation products included thiazole rings, which had characteristic UV absorbances near 245 nm (see **2**, **7**, **8**, and **15,** Figure 4).[12] Other spectroscopic properties associated with thiazoles are three carbon chemical shifts, one near δ 164 (C6) and two between δ 140 and 145 (C2 and C3). Thiazoles with a proton on the carbon between the two heteroatoms, as occurs in the case of **2**,[1] are characterized by low field methine resonances in both the ^{13}C and ^{1}H NMR spectrum (~δ 151 and 8.7, respectively).

As we elucidated these structures, we attempted to rationalize the formation of each with plausible mechanistic degradation pathways. These pathways were helpful in the proposal of the structures of new compounds as they were isolated and characterized spectroscopically, or to propose final details of the molecular structure of the degradation products isolated previously. To allow the direct comparison of NMR chemical shifts throughout the series of isolated products (Table 1), all compounds are numbered in a way that reflects their proposed mechanistic origin from cefaclor, which is numbered as shown in **1**.

Thiazole-Containing Products—The UV spectra of four of the aqueous degradation products were similar to the UV spectrum of **2**[1] (see Figure 4) and other thiazole-containing structures.[12] This similarity was interpreted to indicate of the presence of the thiazole substructure.

Compound ***7***—As shown in Figure 1, **7** is a relatively minor component of the degraded solution, and it has a UV spectrum very similar to that of **2** (λ_{max} ~243 nm). The amount of compound isolated was only sufficient to permit measurement of the ^{1}H NMR and DEPT[7] spectra. These NMR spectra (Table 1) indicated the presence of a phenyl group, thus suggesting the presence of a phenylglycyl substructure. This conclusion was confirmed by the presence of an m/z 106 peak in the mass spectrum. The presence of a sharp singlet at δ 8.57 in ^{1}H NMR spectrum implied the presence of a thiazole with a methine group between the two heteroatoms, as in the case of one of the thiazole rings of **2**.[1] The ^{1}H NMR spectrum

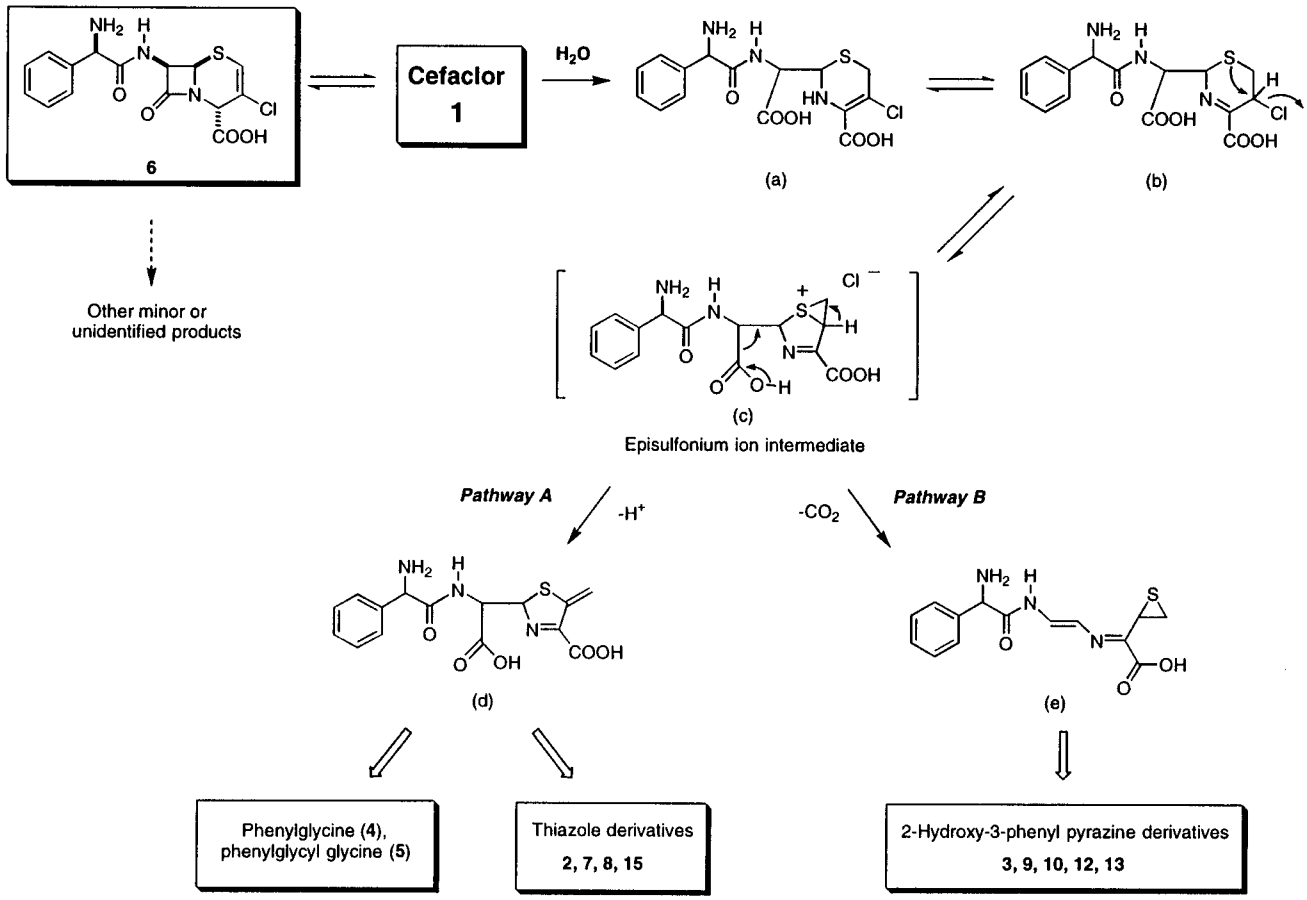

Scheme 1—Generalized acidic degradation pathways of cefaclor.

also showed the presence of a methine (δ 4.57) attached to a methylene (δ 3.71, 3.56). Finally, the methylation experiments discussed later indicated the presence of two carboxylic acids. Hence, the spectroscopic data indicated the partial structures shown at the top of Figure 5.

These substructures account for all the atoms in the molecular formula of the structure, and were used in conjunction with GENOA[13] to obtain the results shown in part in Figure 5. Initial structure generation led to 10 candidate structures. Assuming, based on mechanistic arguments,[1] that one of the carboxylic acid groups would be attached adjacent to the nitrogen of the thiazole ring, the list of candidate structures is reduced to **7**, **7a**, and **7b**, as shown in Figure 5. Considering the initial connectivity of cefaclor and plausible degradation pathways, structures **7a** and **7b** are not feasible. On this basis, and in conjunction with the MS/MS results described later, the structure was assigned as **7**. Assignments for several of the key fragments from the FAB-MS/MS of the protonated molecular ions of **7** and its dimethyl ester are shown below (dimethyl ester fragments denoted by *):

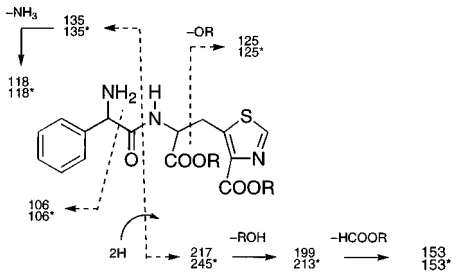

The presence of the *m/z* 106 and 217 (M - 132) fragments confirms the presence of the phenylglycyl moiety. The fragment at *m/z* 106 persists in the dimethyl derivative, whereas *m/z* 217 increases 28 amu to *m/z* 245 upon methylation with diazomethane, indicating the presence of two carboxylic acid groups in this fragment.

Compound ***8***—The mechanistic origins of **2** and **7** (see Scheme 2) suggested that an intermediate thiazole structure, such as **8**, might be formed during the acidic degradation of cefaclor. Examination of the UV spectra of the degradation products (pH 5.5 conditions) obtained from HPLC analysis revealed a minor degradation product eluting at ~9.7 min with a spectrum consistent with a thiazole substructure (λ_{max} 243 nm; see Figure 4). This product was isolated, and analysis by FAB-MS revealed a molecular formula of $C_5H_6NO_3S$ (MH^+, found, *m/z* 160.0081; calc, 160.0068). This molecular formula is consistent with thiazole structure **8**. Derivatization with diazomethane increased the MH^+ to *m/z* 174 (+14 amu), indicating the presence of one carboxyl group. The largest peak in the FAB-MS/MS of the parent compound occurred at *m/z* 142, implying facile loss of water, as might be expected *via* lactonization. The ^1H NMR spectrum acquired in deuterated methanol showed singlets at δ 8.85 (1H) and δ 5.11 (2H), which are reasonable chemical shifts for the protons of the proposed structure.[12] Therefore, the structure of this compound is proposed to be **8**.

Compound ***15***—The fourth thiazole-containing degradation product had a UV λ_{max} of 245 nm (see Figure 4). This product was shown by mass spectrometry to have a molecular formula of $C_{18}H_{19}N_3O_6S$ (found for MH^+, *m/z* 406.1065; calc, 406.1072) and a phenylglycyl moiety (*m/z* 106). From the FAB-MS/MS experiment, other fragments were detected at *m/z* 319, 305, and 273. The fragment at *m/z* 305 is analogous to a fragment in the mass spectrum of another thiazole-containing degradation product, **2**.[1] The fragment at *m/z* 319 suggests an

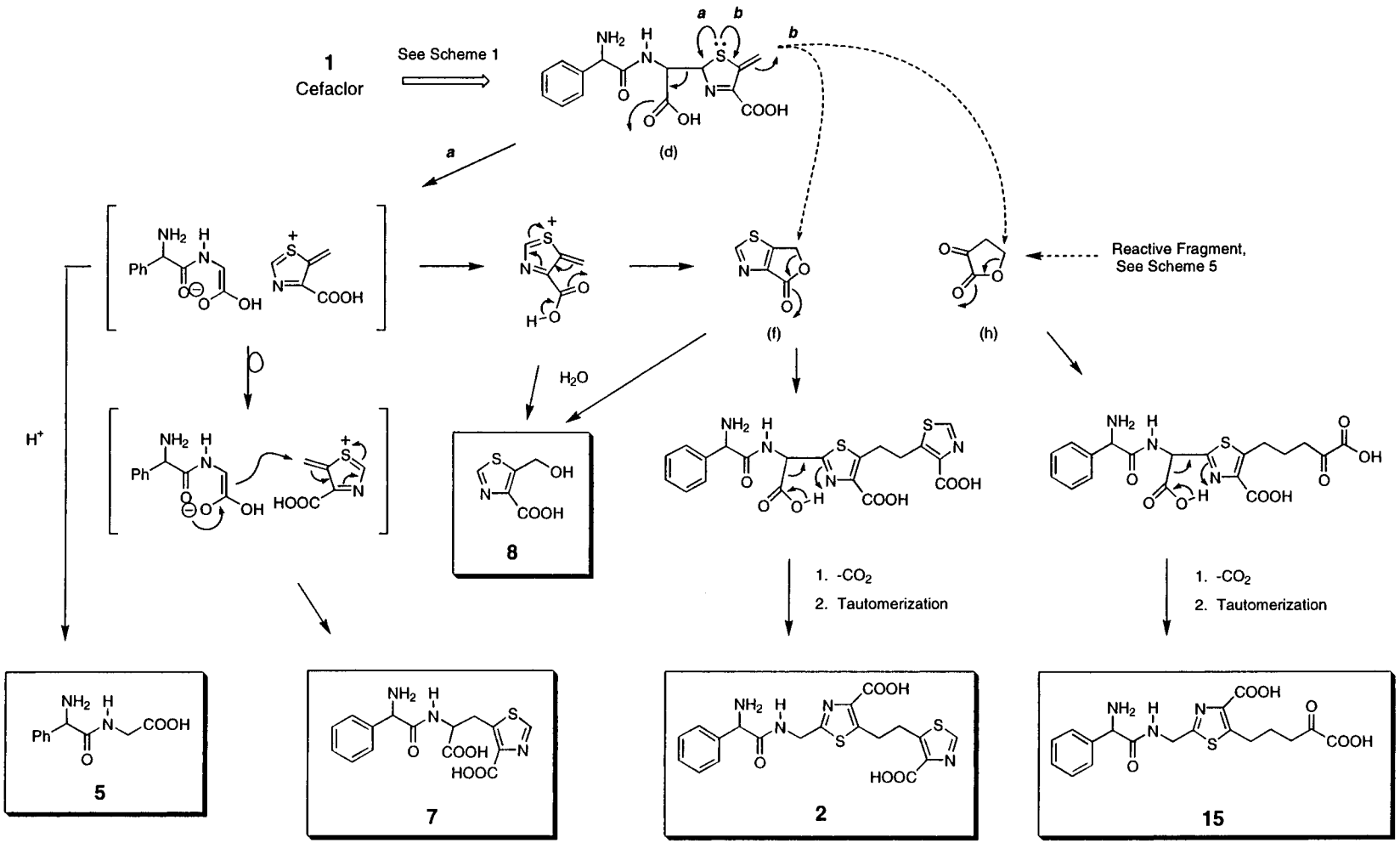

Scheme 2—Pathway A: formation of thiazoles.

additional methylene attached to the *m/z* 305 fragment, and together with the other fragments implies the following partial structure:

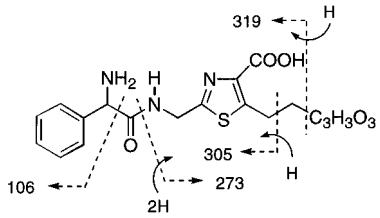

Prior to further spectroscopic characterization, this compound degraded, thus precluding further characterization. However, upon evaluation of the various proposed degradation pathways, the structure of the $C_3H_3O_3$ group can be proposed (see especially Schemes 2 and 5). On this basis, we propose the structure to be **15**. Further work would be needed for conclusive structure elucidation.

"Fluorescent Compounds"—It is well established that β-lactam antibiotics containing the phenyl glycine side chain degrade under certain conditions to yield a highly fluorescent product, 2-hydroxy-3-phenyl pyrazine (2-HPP, structure **3**).[14] In our studies of the acidic degradation of cefaclor, numerous fluorescent products were detected by HPLC with fluorescence detection. Examination of the UV spectra of these products using photodiode array UV detection revealed numerous small peaks (see Figure 1) with spectra similar or identical to that of **3**. Six of these fluorescent degradation products were isolated and characterized. Two of these (**3** and **9**) were reported previously.[14] The mechanistic origin of all of these fluorescent compounds (except for **11**) can be rationalized and generalized on the basis of the pathway shown in Scheme 3. This mechanism permits assignment of the site of substitution on the pyrazine ring, which in some cases is not possible on the available spectroscopic evidence.

*Compound **9***—Accurate mass FAB/MS of **9** (HPLC retention time 16.8 min) revealed an MH^+ of *m/z* 349.1664, which is consistent with a molecular formula of $C_{20}H_{21}N_4O_2$ (calc 349.1665). The UV spectrum of this compound (λ_{max} values of 356 and 253 nm, see Figure 4) is very similar to that of 2-HPP, implying a structural relation between the two compounds. The presence of a 2-HPP substructure was supported by the ^{1}H NMR spectrum (Table 1).

The ^{1}H NMR spectra indicated that the compound contained *two* phenyl groups, but that only one of the two phenyl groups was attached to pyrazine. The mass and NMR spectra clearly showed the presence of a phenylglycyl moiety in the molecule, accounting for the second phenyl group. An amide NH, presumed to be part of the phenylglycyl moiety, was shown by the ^{1}H NMR spectra to be attached to a methylene of an ethylene substructure. These proposals were supported by fragmentations in the mass spectrum of the compound.

The structural information just derived, coupled with GENOA, leads to two candidate structures which differ only by the site of attachment of the methylene group to the pyrazine ring (carbon 6 or 7). On the basis of these results and mechanistic arguments (see Scheme 3) the structure of this compound is proposed to be **9**. This compound has been previously isolated from degradation of ampicillin,[14] and our NMR data are in full accord with those published.

*Compound **10***—The UV of **10** is similar to that of 2-HPP (λ_{max} values of 354 and 246 nm, respectively, see Figure 4). The presence of the 2-HPP substructure was confirmed by the ^{1}H NMR spectrum, which included the relevant pattern of resonances in the aromatic region of the spectrum (*vide supra*). The only other peak in the NMR spectrum was a singlet at δ 3.6 integrating for two protons, indicating the presence of a methylene group. On the basis of accurate mass FAB/MS, the molecular formula of this compound was shown to be $C_{12}H_{10}N_2O_3$ (MH^+: found, 231.0766; calc 231.0770). The FAB-MS/MS spectrum showed significant fragments at *m/z* 185, 157, 104, and 77; the fragment at *m/z* 185 is consistent with the attachment of a methylene group to a 2-hydroxy-3-phenyl pyrazine ring. Thus, structure **10** was proposed. The fragmentation pathway represented next is consistent with the proposed structure.

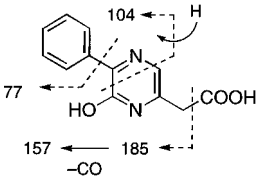

*Compound **11***—This compound, isolated from the degradation in unbuffered water, had a long HPLC retention time (24.7 min), indicating that it was nonpolar relative to most of the other degradation products. The UV spectrum (Figure 4) contained λ_{max} values at 366 and 256 nm. Thus, while the UV spectrum of this product is similar to that of 2-HPP, there is a bathochromic shift of the λ_{max} from the 346 nm absorbance of 2-HPP. Accurate mass EI-MS measurements indicated a molecular formula of $C_{13}H_{12}N_2OS$ (found 244.0637, calc 244.0670). The FAB-MS/MS spectrum (and the EI mass spectrum) showed fragmentation similar to those of the other 2-HPP derivatives.

These results suggest that the structure of this compound includes a 2-HPP group, but with substitution of the pyrazine ring differing from that seen in the other analogs. This conclusion was confirmed by the ^{1}H NMR spectrum. Whereas the qualitative pattern of aromatic resonances typical of these compounds was present, integration showed that only a total of five aromatic protons were present. ^{13}C NMR spectroscopy confirms the presence of these five aromatic protons and that they are in the form of the five sp^2-hybridized methines of a phenyl group. Thus, all aromatic protons are accounted for by the one phenyl group, so that the pyrazine ring must be fully substituted. In addition, the NMR spectra included resonances of three methylene groups, one of which appeared as a singlet (δ 3.75) in the ^{1}H NMR spectrum and the other two of which were mutually coupled (δ 3.12 and 2.99). These data account for a total of 11 of the 12 protons of the molecule. The last proton appeared as a broad singlet below δ 12, attributable to the aromatic hydroxyl proton.

From the aforementioned data, the three substructures in Figure 6 can be deduced. These substructures account for all but the sulfur atom of the molecular formula. As shown by GENOA, only two structures (**11** and **11a**) can result from assembly of these groups. On the basis of mechanistic considerations (see Scheme 4), we propose the structure to be **11**.

*Compound **12***—Compound **12** has a UV spectrum similar to that of 2-HPP (λ_{max} values of 353 and 247 nm). Accurate mass FAB-MS measurements indicated a molecular formula of $C_{14}H_{12}N_2O_3$ (found for MH+, *m/z* 257.0923; calc 257.0926). In the ^{1}H NMR spectrum there appeared the pattern of resonances typical of 2-HPP derivatives. The ^{1}H NMR spectrum contains a five-proton spin system typical of the substructure -CH_2-CH_2-CH<. From the chemical shifts of the protons of the methine (δ 4.12) and the terminal methylene (δ 4.47, 4.35) of this substructure, it is apparent that these carbons bear electronegative substituents. Also present in the ^{1}H NMR spectrum is a broad singlet at δ 7.71. At 80 °C, this resonance is sharpened, but not changed in chemical shift. Furthermore, addition of ^2H_2O to the sample showed that this resonance was not exchangeable.

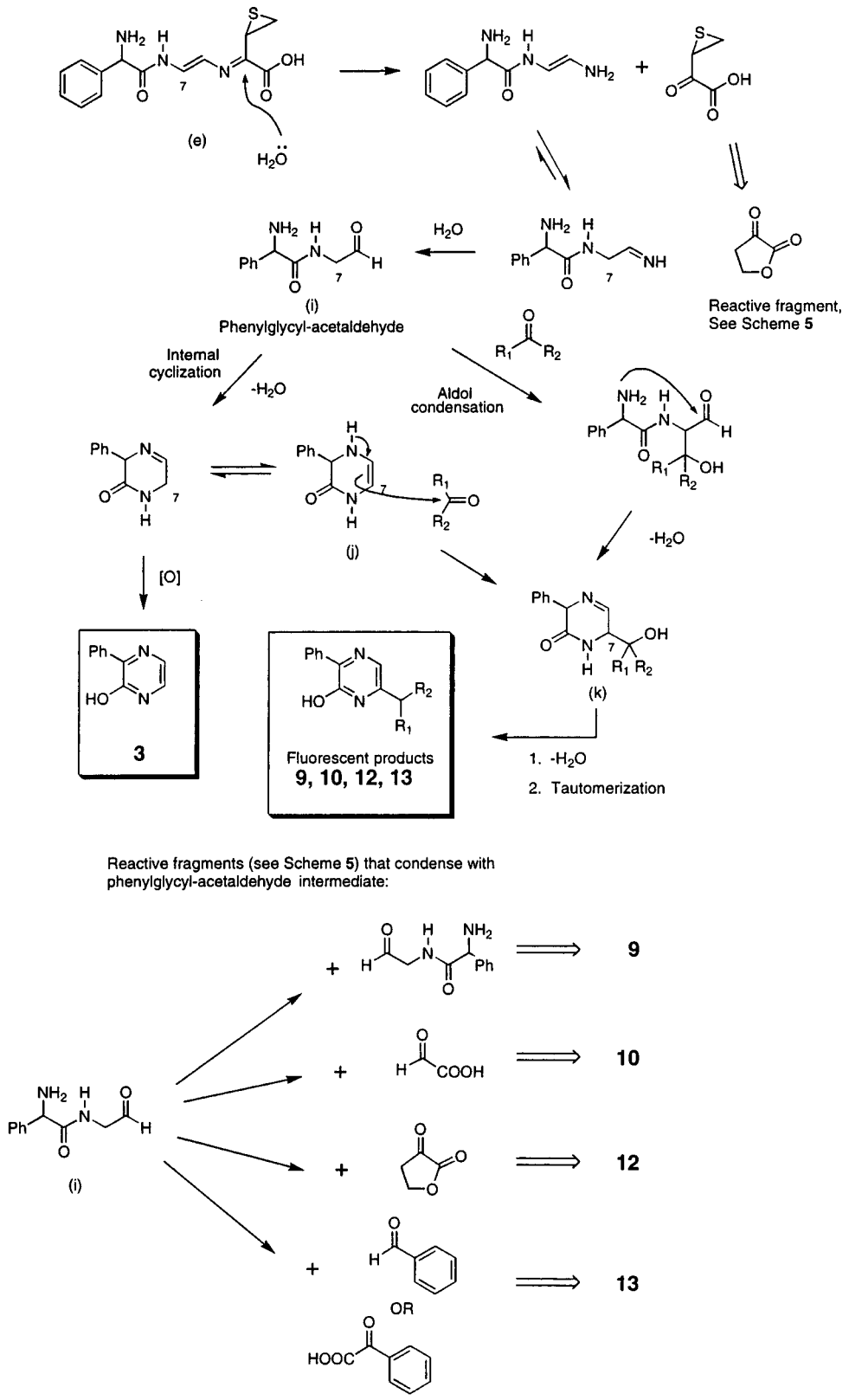

Scheme 3—Pathway B: formation of pyrazine derivatives.

The mass spectrum of the compound includes a significant M-45 fragment, which suggests the presence of a carboxylic acid or a lactone. The compound was shown to react with diazomethane slowly with the uptake of ~1 mol of reagent, a behavior that we have found to be common with hydroxypyrazines. The sluggish reaction of the compound with diazomethane and the fact that the same M−45 loss is seen in the mass spectrum of the methylated derivative indicate that the compound does not contain a free carboxylic acid. This degradation product was therefore proposed to include a lactone substructure.

These substructural constraints, when input into GENOA,

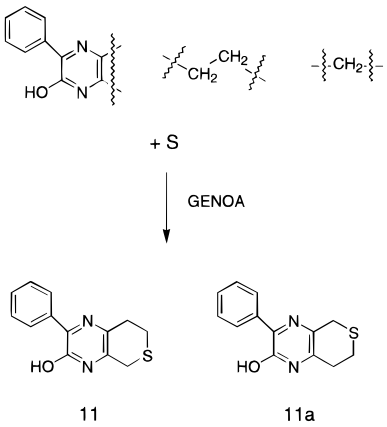

Figure 6—Illustration of the structural possibilities (**11** and **11a**) as determined with the indicated substructural units (derived from spectroscopic characterization) and the computer program GENOA.

result in the construction of only two plausible structures, **12** and **12a**. Of these two candidates, **12** appears to be more consistent with the empirical ^{1}H NMR chemical shifts. The predicted chemical shifts of the methylene protons at sites 2 and 4 in structure **12** are $\sim\delta$ 4,[15] in good agreement with the empirical data. In **12a**, however, the chemical shift of H-2 is predicted to be at significantly higher field ($\sim\delta$ 2.5), as in the case of the analogous site of xanthoquinidin A3.[16] The broad singlet at δ 7.71 can be assigned to H-6 on the pyrazine ring; this singlet is broadened by hindered rotation about the C2-C7 bond, which is possibly accentuated through internal H-bonding from the (protonated) pyrazine nitrogen to the carbonyl group of the lactone. Thus, we propose the structure of the degradation product to be **12**. The electron-impact mass spectral (EI-MS) fragmentation assignments of both the degradation product (R=H) and its monomethyl derivative (R=CH_3*) are represented as follows:

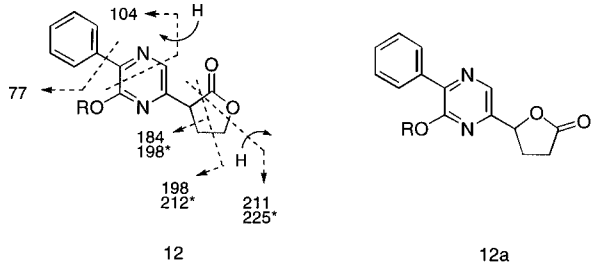

The elemental compositions of all fragment ions shown have been confirmed by accurate mass measurements. Finally, this structure is consistent with the mechanistic proposals described next (see Scheme 3).

*Compound **13***—This relatively nonpolar product ($\sim$25 min HPLC retention time) was isolated from the degradation in water (unbuffered). Compound **13** was postulated to be a derivative of **3** by its UV spectrum (λ_{max} values of 358 and 254 nm, see Figure 4). From accurate mass FAB-MS measurements, the molecular formula for MH^+ was determined to be $C_{17}H_{15}N_2O$ (found *m/z* 263.1182; calc 263.1184). The NMR spectra confirmed that the compound was a 2-HPP derivative and showed that the structure included a second phenyl group and a methylene. Because these substructures account for all the atoms in the molecular formula, the compound can be represented only as a benzyl-2-hydroxy-3-phenylpyrazine. Of the two sites of attachment for the benzyl group (carbons 6 or 7), carbon 7 is selected as the attachment site on the basis of mechanistic arguments as outlined in Scheme 3. This conclusion was confirmed by spectroscopic and chromatographic comparison to a standard.[17]

Miscellaneous Structures—The structures of six of the products isolated in this study were established by comparison with authentic compounds or by reference to previously published data (five of these products are subsequently mentioned and the sixth, **13**, has already been described). Tabulated NMR data for these compounds are presented in Table 1, and UV spectra for **4**, **5**, and **14** are shown in Figure 4.

Sulfur—Elemental sulfur that precipitated from the reaction mixtures was identified by mass spectrometry as described previously.[1]

*Compound **4***—Compound **4** was identified as phenylglycine on the basis of its molecular formula, as established by mass spectrometry. Subsequent chromatographic and spectroscopic comparison to an authentic sample (see *Experimental Section*) confirmed this structure assignment.

*Compound **5***—The structure of **5** (phenylglycylglycine) was proposed on the basis of UV, MS, NMR, and chromatographic retention time by comparison with an authentic sample of the compound. The authentic sample was prepared as described in the *Experimental Section*.

*Compound **14***—The structure of **14** (3-phenyl-2,5-diketopiperazine) was proposed on the basis of its UV and MS spectra, and confirmed by comparison of the ^{1}H NMR spectrum to that described previously.[18] Compound **14** is one of the major degradation products at pH 5.5 and has an HPLC retention time of $\sim$13.4 min.

*Compounds **16** and **17***—One of the earliest eluting preparative HPLC fractions contained a total of four compounds, two of which were identified as **4** and **5** on the basis of MS. Two other minor compounds coeluted with **4** and **5** and, because we were unable to separate these minor compounds from the matrix, their structures (**16** and **17**) have been proposed based on MS.

The FAB-MS spectrum of this fraction showed what appeared to be MH^+ ions at *m/z* 152, 168, 209, 225, and 458. An MS/MS of *m/z* 458 showed that this species was an adduct ion due to the interaction of the *m/z* 152 species with the dispersant used and this ion was not investigated further. Accurate mass determinations on the other peaks in the FAB-MS yielded the elemental compositions shown in Table 2. The peaks at *m/z* 152 and 209 can be assigned to the protonated molecular ions of phenylglycine (**4**) and phenylglycylglycine (**5**), respectively. Those at *m/z* 168 and 225 appear to be the "oxides" of these two compounds.

When the FAB-MS spectrum of this isolate was redetermined using deuterated dispersant, the MH^+ ions were shifted to the masses shown in column 6 of Table 2. These data show that oxidation of phenylglycine and phenylglycylglycine introduces one additional exchangeable proton in each case, thereby ruling out the possibility that the amine functions of these compounds have been oxidized to hydroxylamines. Additionally, it should be noted that the *m/z* 168 and 225 ions lose the elements of ammonia (confirmed by accurate mass measurements) to form *m/z* 151 and 208, respectively, a result that would require the presence of a simple primary amine in these molecules.

The chemically-induced dissociation (CID) mass spectrum of the *m/z* 168 ion taken at 75% primary beam attenuation (to increase the relative intensity of lower mass fragments) clearly showed a fragment at *m/z* 77, indicating that the phenyl ring was not oxidized. A peak at *m/z* 105 in the same spectrum suggests that Ph—C≡O^+ is a fragment of *m/z* 168 and that oxidation occurred on the methine carbon bearing the amino group. The MS results indicate that the structures of the species responsible for the ions at *m/z* 168 and 225 are **16** and **17**, respectively.

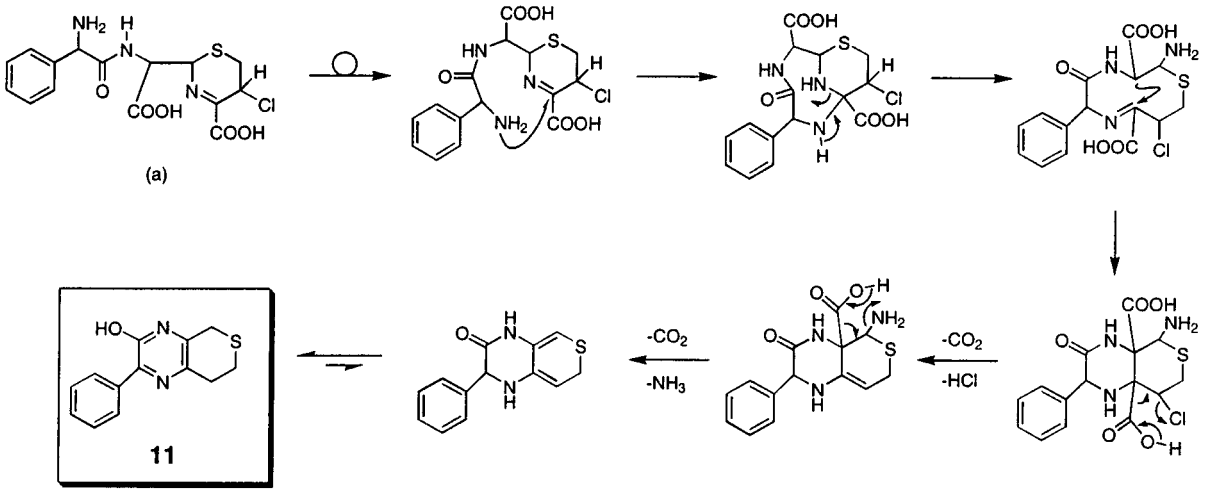

Scheme 4—Formation of pyrazine derivatives **11**.

Table 2—Accurate Mass FAB-MS Measurements on Fraction Containing 4, 5, 16, and 17

Compound	Ion	Found Mass	Composition	Calc. Mass	Deut. Disp[a]	No. Exch
4	*m/z* 152	152.0720	$C_8H_{10}NO_2$	152.0712	156	3
16	168	168.0670	$C_8H_{10}NO_3$	168.0661	173	4
5	209	209.0947	$C_{10}H_{13}N_2O_3$	209.0926	214	4
17	225	225.0889	$C_{10}H_{13}N_2O_4$	225.0610	231	5
Fragment of **17**	208	208.0655	$C_{10}H_{10}NO_4$	208.0610		
Fragment of **16**	151	151.0400	$C_8H_7O_3$	151.0396		

[a]Deuterated dispersant: deuterated "Magic Bullet" (dithiothreitol:dithioerythritol in MeOH).

The isolation of α-hydroxy amino acids such as **16** and **17** seems remarkable considering the expected lability; the loss of ammonia might be expected to proceed rapidly, leading to the resulting ketones. The MS results, however, provide strong evidence supporting these structures. It is noteworthy that α-hydroxy amino acids have been described previously.[19] For example, the 2-hydroxy analog of methionine (also known as methionine hydroxy analogue) has been studied extensively for use as a methionine substitute in animal feeds.[20] We therefore propose that structures **16** and **17** are minor degradation products indicating the presence of a degradation pathway involving benzylic oxidation. This benzylic oxidation pathway is an important part of the mechanistic proposals in both aqueous conditions (see Scheme 5) and in the solid state.[21]

Discussion

X-ray Crystal Structure of Δ^2-Cefaclor—The ORTEP diagram of Δ^2-cefaclor is shown in Figure 7. The absolute configuration of the C4 stereocenter was determined to be *S* by relation to the known stereochemistry of the cefaclor molecule. Few single crystal studies have been performed on Δ^2-isomers of cephalosporin antibiotics. To our knowledge, this is the first instance in which the crystal structures of both the active cephalosporin (i.e., cefaclor[22]) and its respective Δ^2-isomer can be directly compared. In our degradation studies of cefaclor (both aqueous and solid state), we observed the formation of only the 4*S* isomer of Δ^2-cefaclor. Further research would be required to determine whether this selectivity results from kinetic or thermodynamic considerations.

Proposed Degradation Pathways—Previous studies on the degradation of cefaclor by Nakashima et al.[23] suggested that at neutral pH, cefaclor degrades primarily via intramolecular attack of the 11′ primary amine on the β-lactam carbonyl (C8). In a more recent study of the neutral aqueous degradation of cefaclor, Vilanova et al.[24] provided structural evidence for this intramolecular cyclization pathway. Under acidic conditions, however, the nitrogen would be protonated, significantly reducing nucleophilicity. Thus, it is not surprising that this intramolecular cyclization reaction does not appear to be the dominant pathway under acidic conditions. Of all the products isolated in the present study of the acidic degradation of cefaclor, only Δ^2-cefaclor (**6**) retains the β-lactam ring. We therefore propose that acid-catalyzed hydrolysis of this strained ring is, for most of the degradation pathways, the first step in the degradation of cefaclor (see Scheme 1). The various degradation products can be loosely classified into three categories: thiazole derivatives, pyrazine derivatives, and simple hydrolysis or rearrangement products.

*Thiazoles—**8**, **7**, **15**, and **2***—The predominant degradation product contains a thiazole ring, and a mechanism rationalizing the origin of this compound has already been reported.[1] The isolation of three additional thiazole-containing products allows us to generalize this mechanism (see Schemes 1 and 2). The critical intermediate for the pathways leading to thiazole derivatives appears to be (d), which is proposed to form from episulfonium ion intermediate (c) by loss of a proton (Scheme 1). Intermediate (d) can continue the degradation processes in at least two ways. Pathway **a** (Scheme 2) leads to cleavage of the molecule into two moieties that may reorient within a solvent cage, permitting recombination to yield **7**. Escape from the solvent cage leads to the formation of **5** and **8**. Alternatively, intermediate (d) may react as a nucleophile by delivery of the lone pair of electrons on the sulfur atom to the exocyclic methylene group (see Pathway **b**, Scheme 2). In principle, this could lead to reaction with any electrophile in the solution. One such electrophile is **8** or its lactonized form (f) to yield a precursor of compound **2**.[1] Another electrophile that we propose to be present is (h), the reaction of which with intermediate (d) by pathway **b** (Scheme 2) yields the structure proposed for **15**. This mechanism can therefore rationalize the origins of all four of the thiazole-containing products of these degradations, as well as that of **5**.

*Pyrazine Derivatives—**3**, **10**, **13**, **11**, **12**, and **9***—The mechanistic origin of the fluorescent pyrazine degradation products from cephalosporins with a phenylglycyl side chain has already been proposed.[14,25] In Scheme 3, this mechanism is generalized to explain the formations of some minor fluorescent products isolated in this work. The critical intermediate

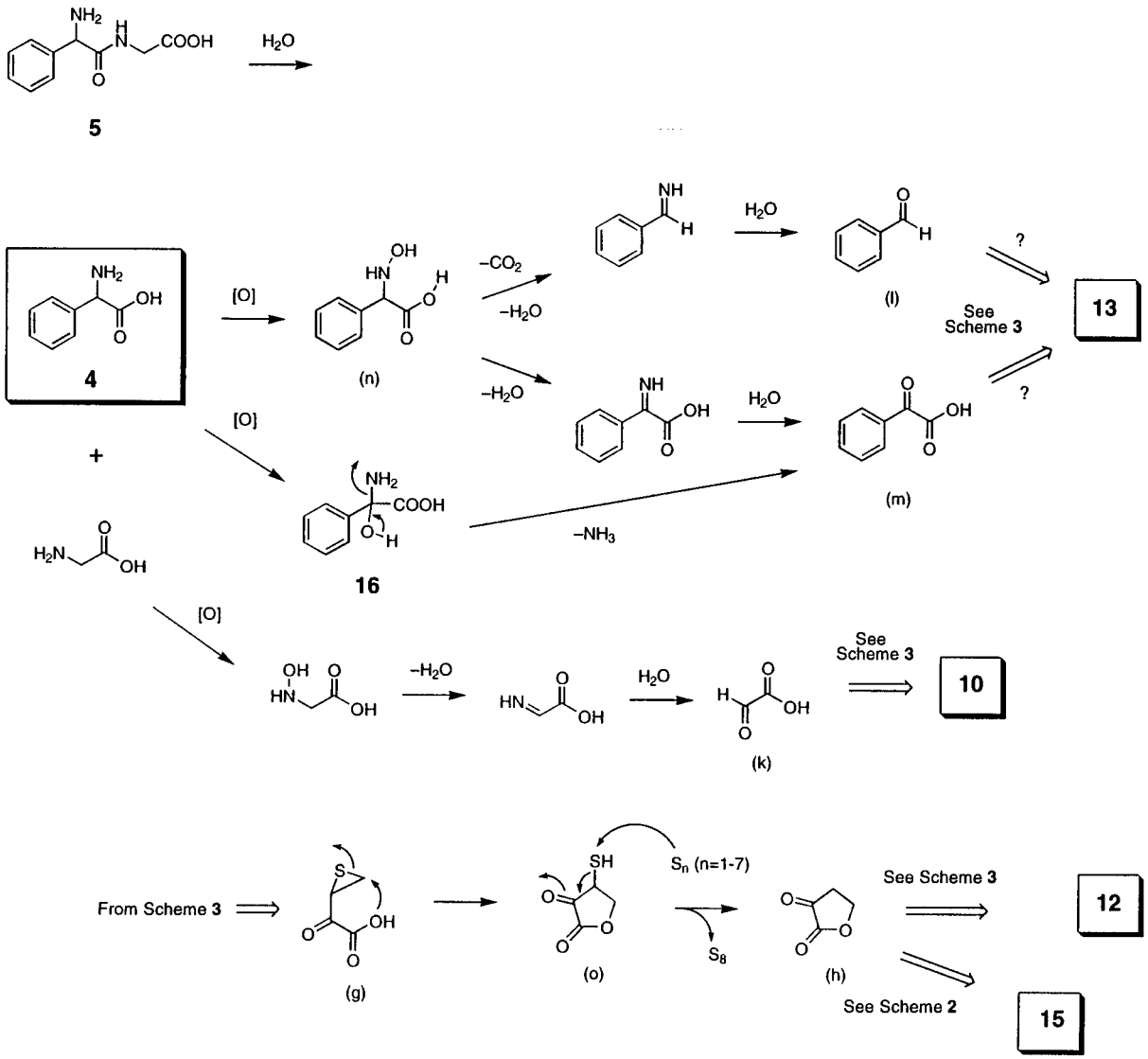

Scheme 5—Formation of reactive "fragments".

is phenylglycyl-acetaldehyde (i), which can be thought of as forming from hydrolysis of (e) as shown in Scheme 3. Different pathways to (i) can be proposed, but any pathway of hydrolysis that reveals the "masked aldehyde" at C6 would suffice. This intermediate can either undergo internal cyclization and oxidation leading to **3**, or it can undergo an aldol condensation with any available electrophiles in the solution. Cyclization, dehydration, and tautomerization lead to the pyrazine derivatives, which differ only in their substitution at C7. Alternatively, the condensation with the electrophilic species could occur *after* internal cyclization.[25] As shown in Scheme 3, the internal cyclization product can tautomerize to form (j), which can react with electrophilic species as shown to form adduct (k); subsequent dehydration and tautomerization leads to the substituted pyrazine derivatives. We have identified five of these substituted pyrazine derivatives (**9**, **10**, **11**, **12**, and **13**), the formation of four of which can be explained with this generalized degradation pathway (**9**, **10**, **12**, and **13**). The formation of **11** involves a novel degradation pathway that does not invoke the formation of a C6 aldehyde (see Scheme 4). An analogous pyrazine derivative, **19**, has been identified as a degradation product of loracarbef, the 1-carba-analog of cefaclor.[26] The proposed degradation pathway to **11** (Scheme 4) is analogous to that proposed for **19**.

An important part of the generalized pathway to pyrazine derivatives is the formation of electrophilic degradation products shown in Schemes 3 and 5. Two products we have isolated (pyrazine **12** and thiazole **15**) appear to be derived from intermediate (h). A structure similar to intermediate (h), structure **18**, was previously isolated as a major acidic degradation product of cephalexin.[2a] In the case of cefaclor, the formation of intermediate (h) is proposed to result from episulfide (g) (Scheme 5) via a reductive nucleophilic attack on thiol (o). The identity of this nucleophile can be proposed by remembering that elemental sulfur is isolated from these degradations. Thus, if the nucleophile is hydrogen sulfide, the presence of which in these degradations is apparent by its odor, a process is started that can lead to elemental sulfur.

Finally, the formation of **10**, **13**, and **15** by the mechanism proposed in Schemes 2 and 3 requires the presence of "electrophilic fragments", such as glyoxylic acid (l) or phenylglyoxylic acid (m), in the degradation mixtures. The formation of these proposed intermediates is shown in Scheme 5. Phenylglyoxylic acid (m) could form via benzylic oxidation of phenylglycine, or through oxidation of the primary amine of phenylglycine to form hydroxylamine (n), followed by dehydration and hydrolysis. The proposed formation of these "electrophilic fragments", although not supported by direct

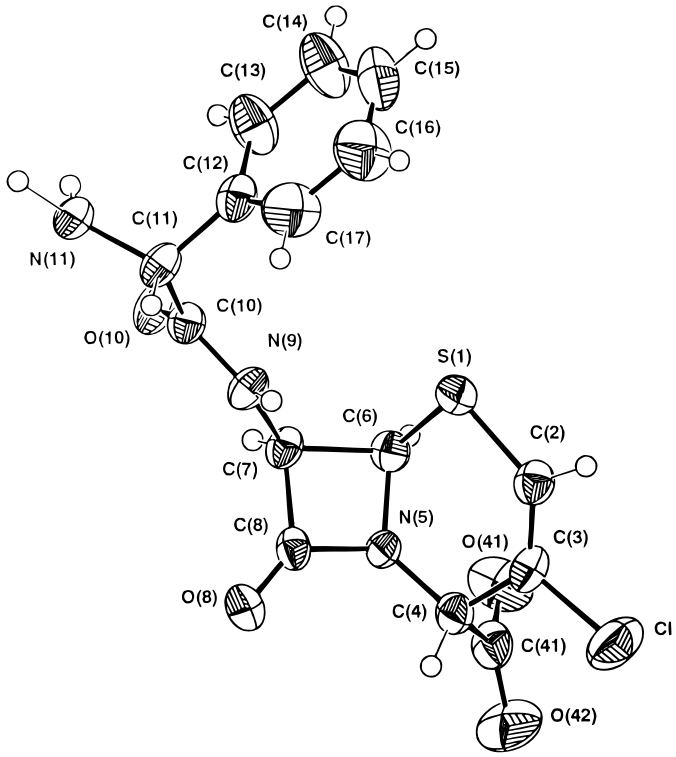

Figure 7—ORTEP diagram of Δ^2-cefaclor. Ellipsoids are drawn at the 50% probability level.

evidence, allows a plausible explanation of the origin of degradation products **10**, **13**, and **15**.

*Simple Hydrolysis or Rearrangement Products—**4**, **14**, **5**, and **6***—Compound **4** (phenylglycine) can arise from a simple hydrolysis of the phenylglycyl-glycine peptide bond. This hydrolysis can occur directly on cefaclor or any of the degradation products or intermediates in which the phenylglycyl side chain is intact. Compound **5** (phenylglycylglycine) can be formed from cleavage of the C6-C7 bond, presumably after β-lactam ring-opening. Although Scheme 2 illustrates the formation of **4** from (d), there are probably multiple "pathways" for this simple cleavage. Compound **6** is the result of a simple tautomerization of the dihydrothiazine double bond. Compound **14** results from an intramolecular nucleophilic attack of the 11′-amine on the β-lactam carbonyl (C8) followed by cleavage of the C6-C7 bond. This nucleophilic attack most likely occurs when the β-lactam is intact rather than after β-lactam hydrolysis.[23] The fact that this compound is a major degradation product at pH 5.5, but was not detected in the acidic degradation solutions is consistent with this hypothesis, because at lower pH, the amine would be more fully protonated and intramolecular nucleophilic attack on the β-lactam carbonyl would not occur when the amine is in the protonated state.

Conclusions

In this study of the aqueous degradation of cefaclor, we have identified more than a dozen degradation products and have proposed several major degradation pathways. This study, while extensive, is not an exhaustive examination of the aqueous degradation pathways of cefaclor. The degradation pathways of cefaclor under neutral and basic pH conditions are complex, essentially unexplored, and remain to be elucidated. The recent study by Vilanova et al.[24] describing a major pathway of cefaclor degradation under neutral conditions provides an excellent start to exploring these degradation pathways. The major solid-state degradation pathways described by Dorman et al.[21] lead to multiple degradation products, many of which are not formed under aqueous conditions. Together, the aqueous and solid-state degradation investigations reveal some of the diverse degradation chemistry of the the cefaclor molecule. Degradation pathways can now be compared with that of loracarbef, the 1-carba analog of cefaclor.[26,27] Evaluation of these aqueous and solid-state degradation pathways reveals the prominent role of the sulfur atom in the degradation of cefaclor.

References and Notes

1. Baertschi, S. W.; Dorman, D. E.; Occolowitz, J. L.; Spangle, L. A.; Collins, M. W.; Wildfeuer, M. E.; Lorenz, L. J. *J. Pharm. Sci.* **1993**, *82*, 622−626.
2. (a) Dinner, A. *J. Med. Chem.* **1977**, *20*, 963; (b) Tai, J., Eli Lilly and Company, unpublished results.
3. Barbhaiya, R. H.; Brown, R. C.; Payling, D. W.; Turner, P. *J. Pharm. Pharmacol.* **1978**, *30*, 224−227.
4. Demarco, P. V.; Nagarajan, R. In *Cephalosporins and Penicillins: Chemistry and Biology*; Flynn, E. H., Ed., Academic: New York; 1972; Chapter 8.
5. Altomare, A.; Cascarano, G.; Giacovazzo, C.; Burla, M. C.; Polidori, G.; Camalli, M. *J. Appl. Crystallogr.* **1994**, *27*, 435.
6. Sheldrick, G. M. "*SHELXS93*: A Program for Crystal Structures Refinement," University of Gottingen, Gottingen, Germany, 1993.
7. Doddrell, D. M.; Pegg, D. T.; Bendall, M. R. *J. Magn. Reson.* **1982**, *48*, 323.
8. Derome, A. E. in *Modern NMR Techniques for Chemistry Research*, Baldwin, J. E., Ed.; Organic Chemistry Series, Pergamon: New York, 1987; Chapter 9.
9. Martin, G. E.; Zektzer, A. S. *Magn. Reson. Chem.* **1988**, *26*, 640−641.
10. Marshall, J. L. In *Carbon-Carbon and Carbon-Proton NMR Couplings: Applications to Organic Stereochemistry and Conformational Analysis*; Marchand, A. P., Ed.; Methods in Stereochemical Analysis; Verlag Chemie International: Deerfield Beach, FL, 1983; Vol. 2, Chapter 2.
11. Porter, Q. N.; Baldas, J. In *Mass Spectroscopy of Heterocyclic Compounds*; Weissberger, A.; Taylor, E. C., Eds.; General Heterocyclic Chemistry; Wiley-Interscience: New York, 1971, p 491.
12. Metzger, J. V.; Vincent, E.-J.; Chouteau, J.; Mille, G. In *Thiazole and Its Derivatives*, Metzger, J. V., Ed.; Wiley Interscience: New York, 1979; pp 5−149.
13. GENOA is a computer program designed to generate all candidate structures consistent with the molecular formula and a given set of substructural constraints; *cf.* Carhart, R. E., *et al., J. Org. Chem.* **1981**, *46*, 1708−1718.
14. Uno, T.; Masada, M.; Kuroda, Y.; Nakagawa, T. *Chem. Pharm. Bull.* **1981**, *29*, 1344−1354.
15. (a) Silverstein, R. M.; Bassler, G. C. *Spectrometric Identification of Organic Compounds*, 1st ed.; Wiley: New York, 1963; appendix B; (b) Smith, S. L. *J. Chem. Ed.* **1977**, *54*, 255.
16. Tabata, N.; Tomoda, H.; Matsuzaki, K.; Omura, S. *J. Am. Chem. Soc.* **1993**, *115*, 8558.
17. The standard of **13** was prepared from the degradation of cephalexin in the presence of benzaldehyde; see *Experimental Section* for details.
18. Kopple, K. D.; Ohnishi, M. *J. Am. Chem. Soc.* **1969**, *91* (4), 962−970.
19. A search of Chemical Abstracts database revealed 15 different patented α-hydroxy amino acid derivatives.
20. Schreiner, C. L.; Jones, E. E. *J. Nutr.* **1987**, *117* (9), 1541−1549.
21. Dorman, D. E.; Lorenz, L. J.; Occolowitz, J. L.; Spangle, L. A.; Collins, M. W.; Bashore, F. N.; Baertschi, S. W. *J. Pharm. Sci.* **1997**, *86*, 540−549 (following paper in this issue).
22. Martinez, H.; Byrn, S. R.; Pfeiffer, R. R. *Pharm. Res.* **1990**, *7* (2), 147−153.
23. Nakashima, E.; Tsuji A.; Nakamura M.; Yamana, T. *Chem. Pharm. Bull.* **1985**, *33*, 2098−2106.
24. Vilanova, B.; Donoso, J.; Muñoz, F.; Garcia-Blanco, F. *Helv. Chim. Acta* **1996**, *79*, 1793−1802.
25. Indelicato, J. M.; Dorman D. E.; Engel, G. L. *J. Pharm. Pharmacol.* **1981**, *33*, 119−121.
26. Baertschi, S. W.; Dorman, D. E.; Spangle, L. A.; Collins, M. S.; Lorenz, L. J. *J. Pharm. Biomed. Anal.* **1995**, *13*, 323−328.
27. Skibic, M. J.; Taylor K. W.; Occolowitz, J. L.; Collins, M. W.; Paschal, J. W.; Lorenz, L. J.; Spangle, L. A.; Dorman, D. E.; Baertschi, S. W. *J. Pharm. Sci.* **1993**, *82* (10), 1010−1017.

Acknowledgments

The authors gratefully acknowledge Dr. Robin D. G. Cooper for helpful suggestions regarding the synthesis of phenylglycylglycine, Mr. Jack Fisher for helpful suggestions regarding the synthesis of **6**, and Dr. Joseph Indelicato and Mr. Gary Engel for providing a sample of **13**. The expert help of Kimmer Smith in carrying out the synthesis of **6** is appreciated.

Supporting Information Available—A description of procedures for crystal data collection and reduction, tables of crystallographic data, and an ORTEP drawing of CEFD (17 pages). Ordering information is given on any current masthead page.

JS960427X